LU TP 95-25
February 19, 1996

Scaling and Scale Breaking in Polyelectrolytes

Carsten Peterson[1], Ola Sommelius[2] and Bo Söderberg[3]
Department of Theoretical Physics, University of Lund
Sölvegatan 14A, S-223 62 Lund, Sweden

Submitted to *Journal of Chemical Physics*

Abstract:

We consider the thermodynamics of a uniformly charged polyelectrolyte with harmonic bonds. For such a system there is at high temperatures an approximate scaling of global properties like the end-to-end distance and the interaction energy with the chain-length divided by the temperature. This scaling is broken at low temperatures by the ultraviolet divergence of the Coulomb potential. By introducing a renormalization of the strength of the nearest-neighbour interaction the scaling is restored, making possible an efficient blocking method for emulating very large polyelectrolytes using small systems.

The high temperature behaviour is well reproduced by the analytical high-T expansions even for fairly low temperatures and system sizes. In addition, results from low-T expansions, where the coefficients have been computed numerically, are presented. These results approximate well the corresponding Monte Carlo results at realistic temperatures.

A corresponding analysis of screened chains is performed. The situation here is complicated by the appearance of an additional parameter, the screening length. A window is found in parameter space, where scaling holds for the end-to-end distance. This window corresponds to situations where the range of the potential interpolates between the bond length and the size of the chain. This scaling behaviour, which is verified by Monte Carlo results, is consistent with Flory scaling. Also for the screened chain a blocking approach can be devised, that performs well for low temperatures, whereas the low-T expansion is inaccurate at realistic temperatures.

[1] carsten@thep.lu.se
[2] ola@thep.lu.se
[3] bs@thep.lu.se

1 Introduction

Thermodynamical properties of uniformly charged polyelectrolytes consisting of linear chains of monomers, with covalent harmonic bonding forces and Coulomb interactions (screened or unscreened), have been extensively studied e.g. with Monte Carlo methods [1, 2, 3, 4, 5, 6] and variational techniques [7, 5]. Less attention has been paid to the low-T and high-T expansions for these systems. To some extent the lack of interest in these two limits has been motivated by the conjecture that "realistic" temperatures fall outside the range of such expansions.

In this work we study the scaling properties of polyelectrolytes starting out from systematic studies of the low-T and high-T expansions both for Coulomb and screened chains. The latter are based upon perturbative treatment of the interaction. Extensive Monte Carlo (MC) calculations are used to evaluate the results.

For the Coulomb chain in dimensionless units there are only two parameters, the number of monomers N and the temperature T. For global quantities such as the end-to-end distance r_{ee} and the interaction energy it turns out that one has approximate scaling for large *rescaled temperatures* $\hat{T} = T/N$. This scaling is broken at low temperatures due to the short-distance divergence of the Coulomb energy. By appropriate renormalization of the harmonic and Coulomb terms and by introducing an additional corrective nearest-neighbor interaction, a blocking scheme results that allows for fairly accurate MC calculations of very large systems with quite modest computational investments [8]. Thus, e.g., when emulating a N=2048 system at room temperature using a system of 50 blocked monomers, approximately a factor 70000 is gained in computing speed at the modest expense of 3.6% error in r_{ee} [8]. At large N the rescaled temperature becomes small and hence one should be able to estimate the thermodynamical quantities using a low-T expansion. Such expansions are systematically developed, and when evaluating the coefficients numerically one is indeed able to compute r_{ee} within 3% for large systems at room temperatures.

For a Debye-Hückel screened chain the situation is quite different. In addition to the parameters N and T one has the Debye screening parameter κ, introducing an additional length scale for the chain. For large κ-values the potential is short range and the chain is essentially Brownian, whereas for low κ the Coulombic chain is recovered. As $N \to \infty$ for fixed (κ, T), scaling relations are obtained, consistent with Flory scaling [9]. When the range of the potential is much larger than the average bond length, but much smaller than the overall chain size, a high temperature expansion indicates a simple dependence on the combination $N/\kappa^4 T^5$ of the deviation from Brownian behaviour, as measured by r_{ee}^2/NT. The blocking approach works reasonably well also for the screened case, at least for relatively low temperatures, despite less firm theoretical foundation. The low-T expansions of global quantities, r_{ee} and the energy, do not provide as accurate results as in the Coulomb case.

Due to the different nature of the unscreened Coulomb and Debye screened chains our presentation is structured such, that each of the two systems is dealt with separately in a self-contained way. We also include in one of the appendices underlying details of the blocking approach of ref. [8].

The paper is organized as follows: In Section 2 the Coulomb model is presented together with scaling and scale breaking properties and numerical results. The corresponding discussion and results for the screened chain can be found in Section 3. In Section 4 a brief summary is given. Most of the details concerning high- and low-T expansions are given in the Appendix A and B respectively.

2 The Coulomb Chain

2.1 The Model

In terms of dimensionless quantities, the energy of a Coulomb chain is given by [5]

$$E^{(N)} \; = \; E_G + E_C \; = \; \frac{1}{2}\sum_{i=1}^{N-1} \mathbf{r}_i^2 + \sum_{\sigma} \frac{1}{r_\sigma} \tag{1}$$

where instead of the absolute monomer positions $\mathbf{x}_i$, the *bond vectors*

$$\mathbf{r}_i \equiv \mathbf{x}_{i+1} - \mathbf{x}_i, \;\; i = 1, \ldots, N-1 \tag{2}$$

are used, and where σ runs over contiguous non-nil sub-chains, with

$$\mathbf{r}_\sigma \equiv \sum_{i \in \sigma} \mathbf{r}_i \tag{3}$$

corresponding to the distance vector between the endpoints of the subchain.

Due to the simple properties of the Hamiltonian under rescaling of the coordinates, the thermal expectation values for E_G and E_C are related by a simple virial identity [5],

$$2\langle E_G \rangle - \langle E_C \rangle \; = \; 3(N-1)T \tag{4}$$

2.2 Zero Temperature

At zero temperature, the polymer is locked in a minimum energy configuration: an aligned configuration with the nearest-neighbour distances b_i satisfying

$$b_i \; = \; \sum_{\sigma \ni i} \frac{1}{b_\sigma^2} \tag{5}$$

To a good approximation, this is solved by

$$b_i \approx \left\{ \log \left(C \frac{i(N-i)}{N} \right) \right\}^{1/3} \tag{6}$$

with $C = \exp(1+\gamma) \approx 4.8$ (γ is Euler's constant ≈ 0.5772). For r_{ee}, E_G and E_C, this implies

$$\begin{aligned} r_{ee} &\approx N \left(\log N\right)^{1/3} \\ E_G &\approx \frac{1}{2} N \left(\log N\right)^{2/3} \\ E_C &\approx N \left(\log N\right)^{2/3} \end{aligned} \tag{7}$$

consistently with the virial identity (eq.(4)) with $T = 0$.

2.3 Low Temperature Expansions

At low temperature, one can make an expansion around the minimum energy configuration. Counting degrees of freedom, removing three for translational invariance and two for rotational symmetry, we have

$$\langle E\rangle \;=\; E_0 + \frac{1}{2}\,(3N-5)\,T + O\left(T^2\right) \tag{8}$$

Using this in combination with the virial identity (eq. (4)), we obtain for the partial energies, E_C and E_G,

$$\begin{aligned}
\langle E_C\rangle \;&=\; \frac{2}{3}E_0 - \frac{2}{3}T + O\left(T^2\right) \\
\langle E_G\rangle \;&=\; \frac{1}{3}E_0 + \left(\frac{3}{2}N - \frac{11}{6}\right) T + O\left(T^2\right)
\end{aligned} \tag{9}$$

The corresponding expansions for the correlations $\langle \mathbf{r}_i \cdot \mathbf{r}_j\rangle$, needed e.g. for r_{ee}, can be found in Appendix A, eq. (A5). These expansions contain coefficients that have to be evaluated numerically.

2.4 High Temperature Expansions

In the high-T limit, the results for r_{ee} and E_C can be expanded in power series in $1/T$. For large N, the first few terms yield (see Appendix B)

$$\begin{aligned}
\langle r_{ee}^2\rangle \;&\approx\; 3NT + \frac{4}{15}\sqrt{\frac{2}{\pi}}\frac{N^{5/2}}{T^{1/2}} \\
\langle E_C\rangle \;&\approx\; \frac{4}{3}\sqrt{\frac{2}{\pi}}\frac{N^{3/2}}{T^{1/2}}
\end{aligned} \tag{10}$$

The corresponding expansion for the bond energy E_G can be obtained from E_C using the virial identity (eq.(4)).

We note that the expressions are consistent with a simple scaling behaviour since for large N both r_{ee}/N and E_C/N are functions of the rescaled temperature, T/N, only. The relevant small parameter of the high-T expansion is obviously N/T. In Appendix B the high-T expansion is discussed in some detail.

2.5 Scaling From a Continuum Formulation

The scaling properties indicated by the high-T expansion can be understood as follows. For large N, we can approximate the discrete polymer by a continuous chain, by rescaling i, $\mathbf{x}_i$ and T,

$$\mathbf{x}_i = N\mathbf{y}\left(\frac{i}{N}\right), \quad T = N\hat{T} \tag{11}$$

in effect replacing the discrete index i by a continuous one, $\tau = i/N$, $0 < \tau < 1$. Then in terms of $\mathbf{y}(\tau)$, the Boltzmann exponent E/T is approximated by $\hat{E}/\hat{T}$, with the *effective continuum*

Hamiltonian $\hat{E}$ given by

$$\hat{E}^{(N)} = \int_0^1 d\tau \frac{1}{2}\dot{\mathbf{y}}(\tau)^2 + \int_0^1 d\tau \int_{\tau+1/N}^1 \frac{d\tau'}{|\mathbf{y}(\tau') - \mathbf{y}(\tau)|} \tag{12}$$

The remaining N-dependence sits entirely in the short-distance cutoff, necessary to prevent a potential logarithmic divergence. Without the cutoff, the following naive scaling behaviour would be exact:

$$\langle E_C \rangle \approx N f(\hat{T}), \quad \langle E_G \rangle \approx \frac{3}{2} N^2 \hat{T} + \frac{1}{2} N f(\hat{T}), \quad \langle r_{ee}^2 \rangle \approx N^2 g(\hat{T}) \tag{13}$$

Indeed, at high $\hat{T}$ the scale-breaking is not important; the singularity is washed out by the Brownian fluctuations. From the high-T expansions above, we infer the asymptotic behaviour of the scaling functions f and g:

$$\begin{aligned} f(\hat{T}) &\approx \frac{4}{3}\sqrt{\frac{2}{\pi}}\hat{T}^{-1/2} + O(\hat{T}^{-2}) \\ g(\hat{T}) &\approx 3\hat{T} + \frac{4}{15}\sqrt{\frac{2}{\pi}}\hat{T}^{-1/2} + O(\hat{T}^{-2}) \end{aligned} \tag{14}$$

At low T, on the other hand, the scaling is more seriously broken:

$$f_N(\hat{T}) \approx (\log N)^{2/3} - \frac{2}{3}\hat{T} \tag{15}$$

2.6 Blocking Degrees of Freedom

Neglecting the residual N-dependence in eq. (12), the scaling properties suggest the possibility of emulating a large system of N monomers by a blocked system of $K = N/Q < N$ effective monomers [8], using the following rescaled Hamiltonian for the latter:

$$E^{(K)}_{\mathrm{B,naive}} = \frac{1}{2Q'} \sum_{i=1}^{K-1} r_{i,i+1}^2 + \frac{3}{2}(N-K)T \; + \; Q^2 \sum_i \sum_{j>i} \frac{1}{|r_{ij}|} \tag{16}$$

where r_{ij} are distances between blocked monomers, each representing Q real monomers, while $Q' = (N-1)/(K-1)$. This simple renormalization technique should work well at high T, where the detailed short-distance properties of the chain are smoothed out by large fluctuations, and less well at low T.

However, the approach can be improved. The N-dependence in the effective continuum Hamiltonian, eq. (12), implies the discrepancy

$$\hat{E}^{(N)} - \hat{E}^{(K)} = \int_0^1 d\tau \int_{\tau+1/N}^{\tau+1/K} \frac{d\tau'}{|\mathbf{y}(\tau') - \mathbf{y}(\tau)|} \tag{17}$$

In the low-T regime, where the chain is more or less linear, the discrepancy is approximately given by

$$\hat{E}^{(N)} - \hat{E}^{(K)} \approx \log(N/K) \int_0^1 \frac{d\tau}{|\dot{\mathbf{y}}(\tau)|} \tag{18}$$

This indicates a possible low-T improvement to the blocking approach: simply add a corrective interaction term corresponding to eq. (18) to the blocked Hamiltonian:

$$E_{\rm B}^{(K)} = E_{\rm B,naive}^{(K)} + \sum_{i=1}^{K} W(r_{i,i+1}) \tag{19}$$

$$W(r) = \frac{Q^2 \log(Q)}{r} \tag{20}$$

With this improved blocked Hamiltonian, very large chains can be emulated (using MC) with relatively small blocked systems with quite small errors all the way down to $T = 0$ [8].

The correction term can also be derived directly for the discrete system by considering eq. (19), with an unspecified corrective nearest-neighbour interaction $W(r)$. At low temperatures we approximate the nearest-neighbour distance by a constant a. For the blocked system, the corresponding nearest-neighbour distance then is $b = Qa$. In this approximation, the Coulomb energy for large N is given by

$$U_N \approx \frac{N}{a} \sum_{l}^{N} \frac{1}{l} \approx \frac{N}{a} \log N \tag{21}$$

while the blocked interaction energy for large K reads

$$U_K \approx \frac{Q^2 K}{b} \log K + K W(b) \tag{22}$$

Choosing $W(r)$ such that $U_N = U_K$ for $b = Qa$ yields precisely eq. (20).

Appendix B contains a discussion of the high-T properties of the blocked system.

2.7 Numerical Comparisons

In this section we compare the results from the high- and low-T expansions as well as scaling properties with MC data. All MC calculations, both for Coulomb and screened chains (see next section) were performed using the pivot algorithm [10]. Most results are based on 10^4 thermalization sweeps and 10^5 measured configurations. Some of the MC results were taken from ref. [5]. For results from exploring the blocking method we refer the reader to ref. [8].

2.7.1 Low T Results

It is of interest to investigate what low T means in terms of physical temperatures. In the dimensionless units of eq. (1), room temperature (290K) corresponds to T_r=0.837808. We have computed r_{ee}/N , where $r_{ee}=\sqrt{\langle r_{ee}^2 \rangle}$, using the low-$T$ expansion corresponding to eq. (A5) for different chain sizes N at $T = T_r$. In fig. 1, comparisons are made between these low-T results and MC data. Also shown in fig. 1 is the T=0 solution (cf. eq. (7)). Not surprisingly the low-T approximation becomes more accurate as N increases since it corresponds to a lower $\hat{T}$. For N=1024 the error is less than 3%, which is quite impressive. Computing r_{ee} for N=1024 using eq. (A5) is $\sim$ 200 times faster than using MC. The computational demand for both methods grows like N^3.

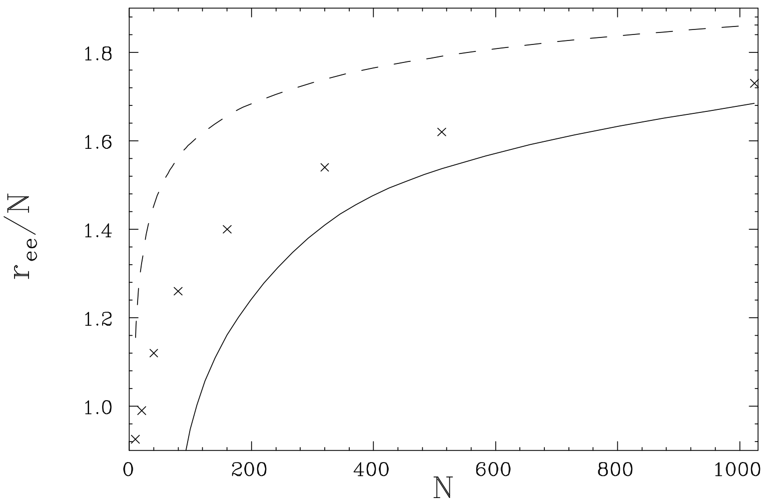

Figure 1: r_{ee}/N as a function of N for a Coulomb chain at $T{=}T_r$. Dashed line, full line and crosses represent $T{=}0$ (eq. (7)), first order low-T expansion (eq. (A5)) and MC results, respectively.

2.7.2 Scaling

Next we test the scaling properties expected from the high temperature expansions (eq. (10) and Appendix B) against numerical results. In figs. 2 and 3, r_{ee}/N and E_C/N are shown as functions of $\hat{T} = N/T$. The predictions from the high-T expansion for r_{ee} fit extremely well for $\hat{T} > 0.2$, whereas for E_C the validity region of this expansion is located at much larger $\hat{T}$. Also shown are the finite-N effects from eqs. (B5,B6), which are larger for E_C than for r_{ee} as can be understood from eqs. (B2,B5,B6). The deviation from scaling in fig. 3 for $\hat{T} > 1$ is almost entirely due to finite-N effects.

3 Debye Screened Chains

Next we turn to the case of the Coulomb chain being screened by the surrounding medium. We model this effect by using the Debye-Hückel potential (being fully aware of its limitations).

3.1 The Model

The energy of the Debye screened chain takes the following form [5]:

$$E(\mathbf{r}) = E_G + E_C = \frac{1}{2}\sum_{i=1}^{N-1} \mathbf{r}_i^2 + \sum_{\sigma} \frac{e^{-\kappa r_\sigma}}{r_\sigma} \tag{23}$$

where the additional parameter κ is the inverse screening length. In what follows we assume that κ is independent of T.

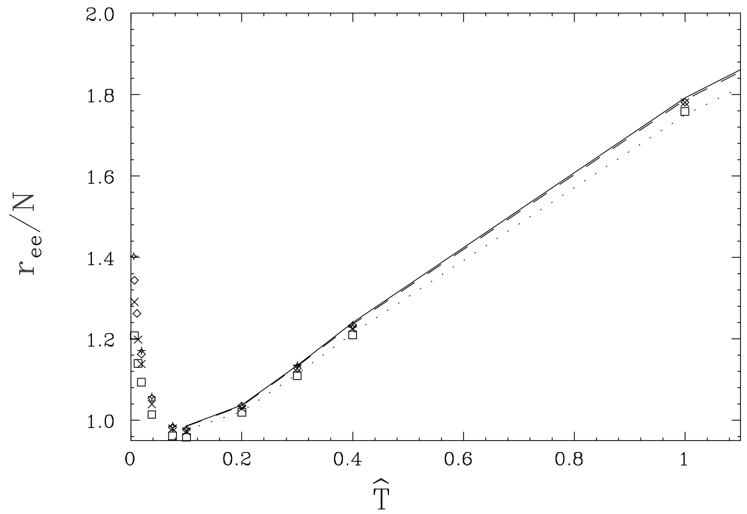

Figure 2: r_{ee}/N as a function of $\hat{T}$ for a Coulomb chain from MC results for N=20 ($\Box$), 40 ($\times$), 80 ($\diamond$) and 160 (+). The lines show second order high-T expansion results for N=20 (dotted), 80 (dashed) and ∞ (full) from eqs. (B5,B6).

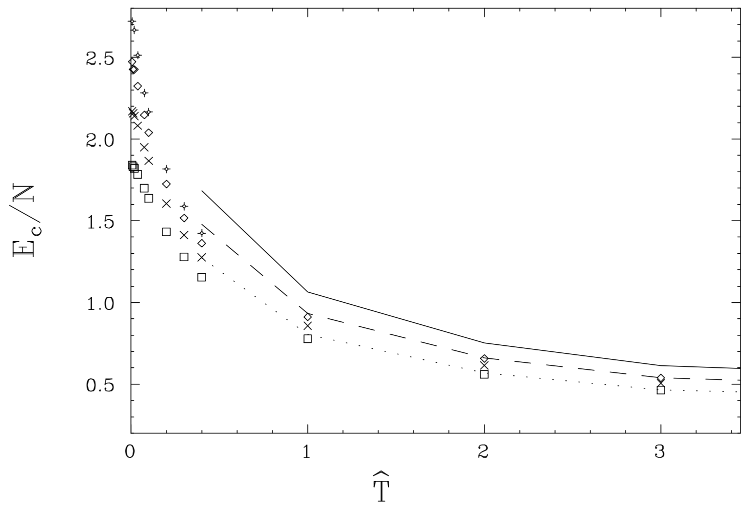

Figure 3: E_C/N as a function of $\hat{T}$ for a Coulomb chain from MC results for N=20 ($\Box$), 40 ($\times$), 80 ($\diamond$) and 160 (+). The lines show leading order high-T results for N=20 (dotted), 80 (dashed) and ∞ (full) from eqs. (B5,B6).

In the screened case, a proper virial identity relating the average bond and interaction energies does not exist (cf. eq. (4)). Still, one has the slightly less useful identity [5].

$$2\langle E_G\rangle - \langle E_C\rangle - \kappa \left\langle \sum_\sigma e^{-\kappa r_\sigma} \right\rangle = 3(N-1)T \qquad (24)$$

3.2 Zero Temperature

Since the screened interaction is short-range, the ground-state configuration can, for large enough N, be considered translation-invariant, with a constant, N-independent nearest-neighbour distance a. Defining $\eta \equiv \kappa a$, we have

$$a^3 = \frac{\eta}{e^\eta - 1} - \log(1 - e^{-\eta}) \tag{25}$$

valid for $N\eta \gg 1$. This gives a implicitly as a function of κ, and we have, for small κ:

$$\begin{aligned} a &\approx (-\log\eta)^{1/3} \\ \kappa &\approx \frac{\eta}{(-\log\eta)^{1/3}} \\ \Rightarrow a &\approx (-\log\kappa)^{1/3} \end{aligned} \tag{26}$$

while for large κ, we obtain

$$\begin{aligned} a &\approx \left((\eta+1)e^{-\eta}\right)^{1/3} \\ \kappa &\approx \frac{\eta}{((\eta+1)e^{-\eta})^{1/3}} \\ \Rightarrow a &\approx 3\frac{\log\kappa}{\kappa} \end{aligned} \tag{27}$$

Similarly, we have for the energy per monomer

$$E_G/N = \frac{a^2}{2} \tag{28}$$

$$E_C/N = -\frac{1}{a}\log\left(1 - e^{-\eta}\right) \tag{29}$$

3.3 Low Temperature Expansions

Also in the screened case, observables can be expanded in a low temperature series, analogous to the Coulomb case, although the details are slightly modified (cf. Appendix A). The expression for $\langle E\rangle$, eq. (8), depends only on the number of degrees of freedom and is still valid, while the expressions for $\langle E_C\rangle$ and $\langle E_G\rangle$ separately (eqs. A12, A13) are less transparent than the corresponding unscreened equations (9).

3.4 High Temperature Expansions

Assuming a T-independent κ, and a large N, we have in the high-T limit

$$\langle r_{ee}^2\rangle \approx 3(N-1)T + 4\sqrt{\frac{2}{\pi}}N^{3/2}\kappa^{-2}T^{-3/2} \tag{30}$$

$$\langle E_C\rangle \approx \zeta(\frac{3}{2})\sqrt{\frac{2}{\pi}}N\kappa^{-2}T^{-3/2} \tag{31}$$

while $\langle E_G \rangle$ in this limit is given by $\frac{3}{2}(N-1)T + \frac{3}{2}\langle E_C \rangle$. In this case, there are no obvious scaling properties.

A Flory estimate of the free energy for the Debye-Hückel potential gives a radius of the chain

$$r \sim \frac{N^{3/5}}{\kappa^{2/5}} \tag{32}$$

indicating that the chain will behave like a self-avoiding walk in the large-N limit. Both Flory scaling and the high temperature expansion, eq. (30), are consistent with a more general scaling behaviour:

$$\frac{r^2}{NT} \sim f\left(\frac{N}{\kappa^4 T^5}\right) \tag{33}$$

where the function $f(x)$ behaves as $3 + 3.2\,x^{1/2}$ for small x, while an asymptotic behaviour $f(x) \sim x^{1/5}$ would correspond to Flory scaling.

Scaling window

A reasonable assumption is that the relevant scaling region is where the range of the potential is small compared to the chain size, and large compared to the monomer-monomer separation, i.e.

$$1 \ll \kappa^2 NT \ll N \tag{34}$$

In this window, the leading expression for $\langle E_C \rangle$, eq. (31), has to be modified into

$$\langle E_C \rangle \approx 2N\kappa^{-1}T^{-1} \tag{35}$$

with $\langle E_G \rangle = \frac{3}{2}(N-1)T + \langle E_C \rangle$, while the expression for $\langle r_{ee}^2 \rangle$, eq. (30), is unaffected.

3.5 Blocking Degrees of Freedom

Despite the fact that the linear chain approximation is of more limited validity in the screened case, one still can devise a blocking approach. Indeed, for low enough temperatures the approach works quite well [8].

In this case the discrete derivation of the correction term is more convenient. Again, starting out from a discrete blocked energy

$$E_{\mathrm{B}}^{(K)} = \frac{1}{2Q}\sum_{i=1}^{K-1} r_{i,i+1}^2 + \frac{3}{2}(N-K)T \; + \; Q^2 \sum_i \sum_{j>i} \frac{e^{-\kappa r_{ij}}}{r_{ij}} + \sum_{i=1}^{K} W(r_{i,i+1}) \tag{36}$$

following the same steps as in the unscreened case, one arrives at

$$W(r) = -\frac{Q^2}{r}\left[\log\left(1 - e^{-\kappa r/Q}\right) - \log\left(1 - e^{-\kappa r}\right)\right] \tag{37}$$

In this way, the longitudinal behaviour will be rather accurately reproduced by the blocked system. However, at low T, the transverse fluctuations will dominate, as indicated by eq. (A8). These are probably more difficult to reproduce than the longitudinal fluctuations.

3.6 Numerical Comparisons

In this section we investigate the validity regime of the high- and low-temperature expansions of r_{ee} for the screened chain. In addition, we test the approximate scaling indicated by eq. (33), and the corresponding scale-breaking arising outside the scaling window given by eq. (34).

In fig. 4 the high- and low-T expansions of the end-to-end distance, eqs. (30, A11), are compared to MC data. Clearly, an increase in κ enlarges the high-T interval and decreases the low-T interval. Quantities at room temperature T_r, for biologically relevant values of κ, are hard to estimate from both high- and low-T expansions.

The approximate scaling as suggested by high temperature expansions and supported by Flory arguments (eq. (33)) is shown in fig. 5 to hold almost too good for the somewhat arbitrary cut $N\kappa^2 T \in (8, 0.3N)$. In fig. 6 the deviation from this behaviour is shown by plotting $\ln(r_{ee}^2/NT)$ as a function of $\ln N\kappa^2 T$ for fixed values of $N/(\kappa^4 T^5)$. Small values of $N\kappa^2 T$ then are equivalent to a high temperature Coulombic limit, while large values ($\gg N$) correspond to a low temperature Gaussian limit. Hence in both limits the curve approaches the Gaussian value, which is $\ln 3$.

A noticeable feature of fig. 6 is the seemingly N-independent rise to the left, indicating that in this region $\langle r_{ee}^2 \rangle$ depends only on $N/\kappa^4 T^5$ and $N\kappa^2 T$, or, equivalently, on $\hat{T} = T/N$ and $\hat{\kappa} = N\kappa$. This is equivalent to stating that a naive (i.e. without the extra nearest-neighbour term) blocking approach should work well there. The scale-breaking seen in the right part of fig. 6, where the curves bend downwards, occurs when $N\kappa^2 T$ becomes comparable to N, violating the assumed scaling condition, eq. (34). For an infinite N, this scale-breaking would be absent, and the corresponding curve would never bend down.

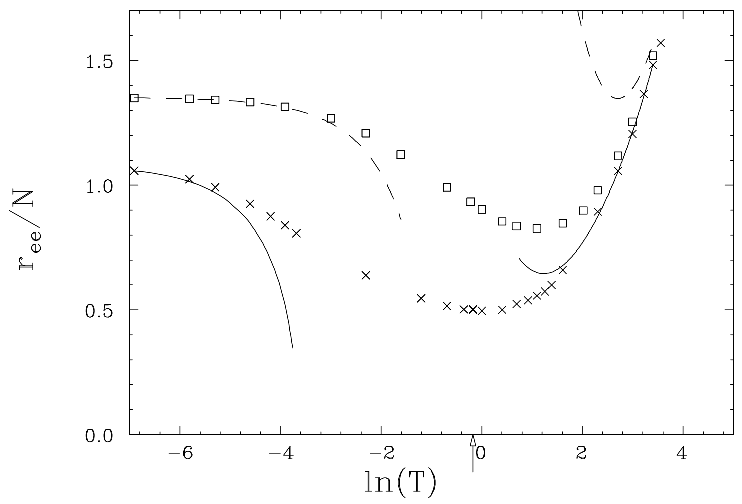

Figure 4: r_{ee}/N as a function of T for a screened, N=40, Coulomb chain with $\kappa = 0.1(\square)$ and 0.63 ($\times$). The lines show second order high-T expansion results (κ=0.1 (dashed), 0.63 (solid)) and the corresponding first order low-T expansions. T_r is marked with an arrow.

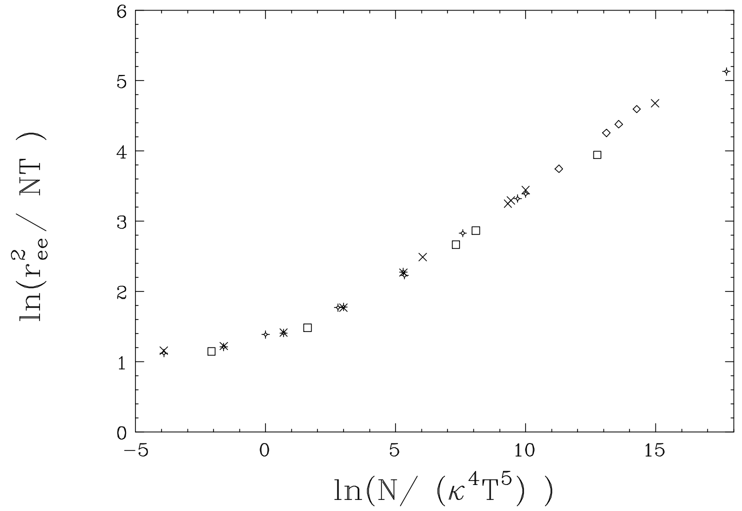

Figure 5: $\ln r_{ee}^2/NT$ as a function of $\ln N/\kappa^4T^5$ with $N\kappa^2T \in (8, 0.3N)$.

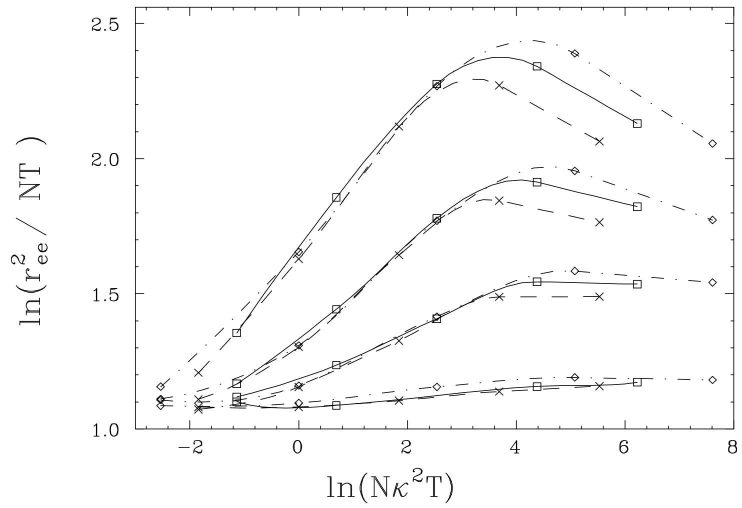

Figure 6: $\ln(r_{ee}^2/NT)$ as a function of $\ln(N\kappa^2T)$. The four collection of curves corresponds to four different values of $\ln N/(\kappa^4T^5)$: from top to bottom 5.30, 2.99, 0.69 and -3.91 for $N = 40(\Box)$, $80(\times)$ and $160(\Diamond)$. The lines are only intended to guide the eye.

4 Summary

Scaling and scale-breaking properties of thermodynamic and conformational properties for simple models of charged polymer chains have been established. These properties are deduced from high- and low-T expansions by means of a perturbative treatment of the interaction for both Coulomb and Debye-Hückel screened chains. In addition to the naive high-T limit with fixed κ for the screened chains we also consider a restricted limit where $T \to \infty$ and $\kappa \to 0$ while keeping $N\kappa^2T$ large and κ^2T small.

For the Coulomb chain, an increase in N makes the chain stiffer due to the long-range character of the electrostatic interaction. The same effect is obtained by lowering the temperature; indeed, thermodynamic quantities for long chains are well approximated by a low-temperature expansion. The relevant variable of the chain is the rescaled temperature $\hat{T} = T/N$, as further supported by high-T expansions which for large N become equivalent to high-$\hat{T}$ expansions.

For the screened chain the situation is somewhat different due to the appearance of a new length scale – the inverse screening length κ^{-1}. For κ^{-1}-values in a window between the bond length and the chain length, a relevant scaling variable $N/(\kappa^4 T^5)$ can be identified. The associated scaling behaviour is consistent with Flory scaling [9].

The scaling properties in terms of $\hat{T} = T/N$ provides a firm theoretical basis for the real space blocking scheme of ref. [8]; a detailed derivation is given. As reported in ref. [8] this approach is very powerful for computing r_{ee} and E_C, both for Coulomb and screened chains, with low errors. Nothing prohibits the extension of the blocking scheme to include titration and multi-chain systems.

For relatively small temperatures, the low-T expansion from ref. [5] is further developed into an efficient computational tool for computing conformational properties. In the Coulomb case results at room temperatures with low errors emerge from this scheme. For the screened case the low-T approach is not viable, at least for reasonable values of N, T and κ.

Appendix A. Low T Expansions

Coulomb Chains

This section has a certain unavoidable overlap with Appendix D in ref. [5]. Low-T expansions for $\langle E_C \rangle$ and $\langle E_G \rangle$ are given in eq. (9). Computing low-T corrections to r_{ee} is somewhat more elaborate.

In terms of the zero temperature bond lengths defined by $b_i \equiv \sum_{\sigma \ni i} \frac{1}{b_\sigma^2}$ we define a set of tensors

$$B_{ij} = \sum_{\sigma \ni i,j} \frac{1}{b_\sigma^3} \tag{A1}$$

$$C_{ijk} = \sum_{\sigma \ni i,j,k} \frac{1}{b_\sigma^4} \tag{A2}$$

In addition, we need the two matrices related to B,

$$U = (1+2B)^{-1} \tag{A3}$$

$$V = P(1-B)^{-1}P \tag{A4}$$

where P denotes the projection matrix onto the subspace orthogonal to b, which is a zero-mode of $1-B$.

In terms of these tensors, we have the quadratic expectation-values at low-T:

$$\langle \mathbf{r}_i \cdot \mathbf{r}_j \rangle = b_i b_j + T\left(U_{ij} + 2V_{ij} + \frac{4 b_i b_j}{3\sum_k b_k^2} + 3\sum_{klm} C_{klm}(b_i U_{jk} + b_j U_{ik})(U_{lm} - V_{lm}) \right) + O(T^2) \tag{A5}$$

where the first two terms of the T coefficient are the naive contributions from the longitudinal and transverse fluctuations. The rest are corrections due to the rotational degeneracy of the $T=0$ configuration, which is also responsible for the transverse zero-modes (of $1-B$). In terms of this expression, $\langle r_{ee}^2 \rangle$ is obtained by summing independently over i and j, while $\langle E_G \rangle$ is obtained by summing over $i=j$ and dividing by two.

Screened Chains

For a screened chain, with b_i still denoting the (now κ dependent) zero temperature bond lengths, the tensors take the following form

$$B = \sum_{\sigma \ni i,j} \frac{e^{-\kappa b_\sigma}}{b^3}(1+\kappa b_\sigma) \tag{A6}$$

$$U = \left(1 + \kappa^2 \sum_{\sigma \ni i,j} \frac{e^{-\kappa b}}{b_\sigma} + 2B \right)^{-1} \tag{A7}$$

$$V = P(1-B)^{-1}P \tag{A8}$$

while two versions of the C-tensor are needed, one related only to parallel fluctuations $C^{(ppp)}$ and the other, $C^{(ptt)}$, coupled to one parallel and two transverse fluctuations.

$$
\begin{aligned}
C_{ijk}^{(ppp)} &= \sum_{\sigma\ni i,j,k} \frac{e^{-\kappa b}}{b^4}\left(1+\kappa b+\frac{\kappa^2 b^2}{3}\right) && \text{(A9)}\\
C_{ijk}^{(ptt)} &= \sum_{\sigma\ni i,j,k} \frac{e^{-\kappa b}}{b^4}\left(1+\kappa b+\frac{\kappa^2 b^2}{2}+\frac{\kappa^3 b^3}{6}\right) && \text{(A10)}
\end{aligned}
$$

In terms of these tensors we have, to first order in the low-T expansion, the expectation values

$$
\langle \mathbf{r}_i\cdot\mathbf{r}_j\rangle = b_i b_j + T\left(U_{ij}+2V_{ij}+2\frac{\sum_k b_k\left(b_j U_{ik}+b_i U_{jk}\right)}{\sum b_k^2}+3\sum_{klm}\left(C_{klm}^{(ppp)}U_{lm}-C_{klm}^{(ptt)}V_{lm}\right)\left(b_j U_{ik}+b_i U_{jk}\right)\right) \tag{A11}
$$

$$
\begin{aligned}
\langle E_C\rangle &= \sum_\sigma \frac{e^{-\kappa b}}{b} - T\sum_i\left(2\frac{\sum_j b_i b_j U_{ij}}{\sum b_k^2}+3\sum_{klm}\left(C_{klm}^{(ppp)}U_{lm}-C_{klm}^{(ptt)}V_{lm}\right)b_i U_{ik}\right)\\
&\quad -\frac{T}{2}\left(\mathrm{Tr}\ U+2\mathrm{Tr}\ V\right)+\frac{3N-5}{2}T && \text{(A12)}\\
\langle E_G\rangle &= \frac{1}{2}\sum_i b_i^2 + T\sum_i\left(2\frac{\sum_j b_i b_j U_{ij}}{\sum b_k^2}+3\sum_{klm}\left(C_{klm}^{(ppp)}U_{lm}-C_{klm}^{(ptt)}V_{lm}\right)b_i U_{ik}\right)\\
&\quad +\frac{T}{2}\left(\mathrm{Tr}\ U+2\mathrm{Tr}\ V\right) && \text{(A13)}
\end{aligned}
$$

Appendix B. High T Expansions

Sums at large N

In what follows, we will encounter sums over subchains like the following for large N

$$S_\alpha \equiv \sum_\sigma L_\sigma^\alpha \equiv \sum_{k=1}^{N}(N-k)k^\alpha \tag{B1}$$

where L_σ is the length (i.e. the number of bonds) of the subchain σ. Obviously, there exist $N-k$ distinct subchains of length k.

In particular, we will encounter the following sums:

$$\begin{aligned} S_{1/2} &= \frac{4}{15}N^{5/2} + BN - \frac{1}{12}N^{1/2} - A + \ldots \\ S_{-1/2} &= \frac{4}{3}N^{3/2} + CN - B - \frac{1}{12}N^{-1/2} + \ldots \\ S_{-3/2} &= DN - 4N^{1/2} - C - \frac{1}{12}N^{-3/2} + \ldots \end{aligned} \tag{B2}$$

where the numerical values of the constants A, B, etc. are

$$A \approx -.02548, \quad B \approx -.20789, \quad C \approx -1.46035, \quad D \equiv \zeta(3/2) \approx 2.612375 \tag{B3}$$

In addition, we need

$$\zeta(3) \approx 1.202057 \tag{B4}$$

High T expansions for a Coulomb chain

For a system of N monomers, we have the following high-T expansions, which are obtained by considering the Coulomb interaction as a perturbation,

$$\begin{aligned} \langle r_{ee}^2 \rangle &\approx 3(N-1)T + \sqrt{\frac{2}{\pi}}T^{-1/2}\sum_\sigma L_\sigma^{1/2} \\ \langle E_G \rangle &\approx \frac{3}{2}(N-1)T + \frac{1}{2}\sqrt{\frac{2}{\pi}}T^{-1/2}\sum_\sigma L_\sigma^{-1/2} \\ \langle E_C \rangle &\approx \sqrt{\frac{2}{\pi}}T^{-1/2}\sum_\sigma L_\sigma^{-1/2} \end{aligned} \tag{B5}$$

At large N these simplify to

$$\begin{aligned} \langle r_{ee}^2 \rangle &\approx 3(N-1)T + \frac{4}{15}\sqrt{\frac{2}{\pi}}T^{-1/2}N^{5/2} \\ \langle E_G \rangle &\approx \frac{3}{2}(N-1)T + \frac{2}{3}\sqrt{\frac{2}{\pi}}T^{-1/2}N^{3/2} \\ \langle E_C \rangle &\approx \frac{4}{3}\sqrt{\frac{2}{\pi}}T^{-1/2}N^{3/2} \end{aligned} \tag{B6}$$

The corresponding high-T expansions for a blocked system ($N \to K = N/Q$) yield identical expressions to the order shown, as long as K is large. This can be understood by considering the blocked Hamiltonian of eq. (19), with E_G defined to include the constant $\frac{3}{2}(N-K)T$, and E_C to include the corrective nearest-neighbour interaction. The latter term, given by eq. (20), does not contribute in the high-T limit: it is needed only at low T.

Generic Perturbation Expansion for Screened Chain

For a Debye screened chain, one must distinguish between two distinct high-T limits – (1) the naive one, where $T \to \infty$ with a constant κ, and (2) a modified limit, corresponding to the scaling window, eq. (33), where $T \to \infty$ and $\kappa \to 0$ keeping $\kappa^2 T$ small and $N\kappa^2 T$ large. The latter of course requires a large N.

In both cases the analysis is based on a perturbative treatment of the interaction, which to a few orders yields the following results for a screened chain of N monomers.

$$\begin{aligned} \langle r_{ee}^2 \rangle &\approx 3(N-1)T + \sqrt{\frac{2}{\pi}}\kappa^3 T \sum_\sigma L_\sigma^2 F_2(\kappa\sqrt{L_\sigma T}) \\ \langle E_G \rangle &\approx \frac{3}{2}(N-1)T + \frac{1}{2}\sqrt{\frac{2}{\pi}}\kappa^3 T \sum_\sigma L_\sigma F_2(\kappa\sqrt{L_\sigma T}) \\ \langle E_C \rangle &\approx \sqrt{\frac{2}{\pi}}\kappa \sum_\sigma F_1(\kappa\sqrt{L_\sigma T}) \end{aligned} \tag{B7}$$

where the $F_k()$ are erf-related functions, defined by

$$F_k(x) = (2k-1)!!\exp(x^2/2)\int_x^\infty dy\, y^{-2k}\exp(-y^2/2) \tag{B8}$$

Conventional High T expansion for a Screened Chain

In the $T \to \infty$ limit with a constant κ and a fixed large N, the sum in the expression for $\langle r_{ee}^2 \rangle$ is dominated by the large L terms (scaling) and can be approximated by an integral. In contrast, the sums in $\langle E_C \rangle$ and $\langle E_G \rangle$ are dominated by small L (no scaling), and must be explicitly summed. We thus obtain

$$\begin{aligned} \langle r_{ee}^2 \rangle &\approx 3(N-1)T + 4\sqrt{\frac{2}{\pi}}N^{3/2}\kappa^{-2}T^{-3/2} \\ \langle E_G \rangle &\approx \frac{3}{2}(N-1)T + \frac{3}{2}\langle E_C \rangle \\ \langle E_C \rangle &\approx \zeta(\frac{3}{2})\sqrt{\frac{2}{\pi}}N\kappa^{-2}T^{-3/2} \end{aligned} \tag{B9}$$

The corresponding high-T expansions for a blocked system, based on eqs. (36, 37) with large K

and large Q, yield for $\langle r_{ee}^2 \rangle$ the same as above. However, $\langle E_G \rangle$ and $\langle E_C \rangle$ become too large,

$$\begin{aligned} \langle E_G \rangle &\approx \frac{3}{2}(N-1)T + \frac{3}{2}\langle E_C \rangle \\ \langle E_C \rangle &\approx \sqrt{\frac{2}{\pi}}\zeta\left(\frac{3}{2}\right) N\kappa^{-2}T^{-3/2}\left(Q^{-1/2} + \frac{\zeta(3)}{\zeta(\frac{3}{2})}Q^{3/2}\right) \end{aligned} \tag{B10}$$

This is due to an overshooting by the corrective term, eq. (37), which gives rise to the $Q^{3/2}$ term in the expression for $\langle E_C \rangle$. On the other hand, upon omitting the corrective term, $\langle E_C \rangle$ becomes too small by a factor $Q^{-1/2}$, due to the lack of scaling mentioned above. Obviously, for thermodynamic properties, the blocking method does not apply in this limit.

Modified High T expansion for Screened Coulomb

With the restriction of staying within the scaling window, $\kappa^2 T \ll 1 \ll N\kappa^2 T$, all three sums scale, i.e. they are dominated by the large-L terms. While the expression for $\langle r_{ee}^2 \rangle$ remains unchanged, we obtain for $\langle E_G \rangle$ and $\langle E_C \rangle$ in this limit

$$\begin{aligned} \langle E_G \rangle &\approx \frac{3}{2}(N-1)T + \langle E_C \rangle \\ \langle E_C \rangle &\approx 2N\kappa^{-1}T^{-1} \end{aligned} \tag{B11}$$

For a system blocked into K effective monomers, these expressions are reproduced, provided also the blocked system is in the scaling window, i.e. if $\kappa^2 TQ \ll 1$; otherwise it yields to too small values for $\langle E_C \rangle$ and $\langle E_G \rangle$.

References

[1] G. A. Christos and S. L. Carnie, *J. Chem. Phys.* **91**, 439 (1089).

[2] H.H. Hooper and H.W. Blanch and J. M. Prausnitz, *Macromolecules* **23**, 4820 (1990).

[3] P.G. Higgs and H. Orland *J. Chem. Phys.* **95**, 4506 (1991).

[4] M. Ullner and B. Jönsson and P.-O. Widmark, *J. Chem. Phys.***100**, 3365 (1994).

[5] B. Jönsson, C. Peterson and B. Söderberg, *J. Phys. Chem.* **99**, 1251 (1995).

[6] M.J. Stevens and K. Kremer, *J. Chem. Phys.* **1669**, 4 (1995).

[7] B. Jönsson, C. Peterson and B. Söderberg, *Phys. Rev. Lett.* **71**, 376 (1994).

[8] C. Peterson, O. Sommelius and B. Söderberg, *Phys. Rev. Lett.* **76**, 1079 (1996).

[9] P.J. Flory, *J. Chem. Phys.* **17**, 303 (1949).

[10] M. Lal, *Mol. Phys.* **17**, 57 (1969);
N. Madras and A.D. Sokal, *J. Stat. Phys.* **50**, 109 (1988). **50**, 109 (1988).

[11] A. Irbäck, *J. Chem. Phys.* **101**, 1661 (1994).